Supporting Materials

Glial cell line-derived neurotrophic factor (GDNF) mediates hepatic stellate cell activation via ALK5/Smad signaling

Le Tao[#1,2], Wenting Ma[#2], Liu Wu[#2], Mingyi Xu[#3], Yanqin Yang[4], Wei Zhang[1], Wenjun Sha[5], Hongshan Li[6], Jianrong Xu[7], Rilu Feng[8], Dongying Xue[2], Jie Zhang[2], Steven Dooley[8*], Ekihiro Seki[9*], Ping Liu[10,11*], Cheng Liu[1,2,12*]

Reagents

α-SMA (A5228) was purchased from Sigma (Saint Louis, MO, USA); the GDNF ELISA kit (DY212), recombinant GDNF cytokine (212-GD), recombinant TGF-β1 (240-B-002), ALK-5 Fc chimera (cat. 3025-BR) and ALK5 (AF3025, for laser confocal microscopy) were purchased from R&D (Minneapolis, MN, USA). The phospho-Akt pathway antibody sample kit (9916), Ret (14556), p-Smad3 (9520), and Smad3 (9523) were purchased from CST (Boston, MA, USA). Smad2 (ab71109), p-Ret (ab51103), p-Smad2 (ab53100), Col 1 (ab138492), GDNF (ab18956 for laser confocal microscopy, immunoblotting, IP, and for treatment on mice) and ALK5 (ab31013, for immunoblotting and IP), DoubleStain IHC kit (ab210059 for human samples and ab183273 for mouse samples), α-SMA (ab5694 for dual staining), mouse specific HRP/DAB Detection IHC kit (ab 64259) were from Abcam (Cambridge, MA, USA). GFRα1 (sc-271546 for immunoblots), and RPI-1 (sc-255524, an inhibitor of Ret), GDNF (sc-13147 for immunohistochemistry, dual staining and for treatment mice) were from Santa Cruz (Dallas, TX, USA). MK-2206 2HCl (Akt inhibitor), SB431542 (TβRI inhibitor) and LY2157299 (galunisertib, TβRI inhibitor), Levamisole hydrochloride (S1939) were obtained from Selleck (Shanghai, China). Biotinylated anti-rabbit IgG (BA-100) and Vectastain ABC kit were purchased from Vector Laboratories (Burlingame, CA, USA). GDNF adenovirus (093692A) and Gdnf sgRNA CRISPR/Cas9 adenovirus (K4921721) were purchased from Abm (Richmond, BC, Canada). The pc-DNA3-ALK5-WT plasmid (#80867) was purchased from Addgene (Cambridge, MA, USA). The KOD-plus-mutagenesis kit (SMK-101 20

reactions) was purchased from Toyobo (Osaka, Japan). The rabbit IgG antibody was purchase from Proteintech (cat. B900610, Rosemont, IL, USA) used as control Ab treatment on mice.

Hepatic stellate cell isolation and culture

The human HSC cell line LX-2 (cat. SCC640) was purchased from Merck (Darmstadt, Germany), and cultured in Dulbecco's Modified Eagle's Medium (DMEM) supplemented with 2% FBS and 1% penicillin streptomycin antibiotics. Human (h) HSCs (hHSCs, cat. #5300), hepatocytes (cat. #5200), hepatic macrophages (hKCs) (cat. #5340), and hepatic sinusoidal endothelial cells (hLSECs) (cat. #5000) were purchased from ScienCell Research Laboratories (San Diego, CA, USA). Human hepatocytes were cultured in MEM199 supplemented with 10% FBS. Human KCs were cultured in RMPI1640 supplemented with 10% FBS. Human LSECs were cultured in endothelial cell medium (cat. #1001) supplemented with 10% FBS.

Primary HSCs, Kupffer cells, and LSECs were isolated from mice by *in situ* liver perfusion with pronase E (cat. 11459643001, Roche, Mannheim, German) and collagenase D (cat. V900893, Vetec, Shanghai, China), followed by density gradient centrifugation with Nycodenz (cat. 1002424, Oslo, Norway), as described elsewhere [1].

KCs were purified by density gradient centrifugation with Nycodenz (9.5% over

14.5%) at 1400 g and 25 ℃, for 22 minutes, which produced a KC-enriched fraction in the middle whitish layer. Purification was achieved by allowing the cells to adhere to plastic culture plates at 37 ℃ for 20 minutes, and nonadherent cells were removed by washing, as previously reported [2]. For activated HSCs, cells were maintained in DMEM supplemented with 10% FBS and 1% antibiotic-antimycotic (cat. 15420-062. Gibco, NY, USA) for 7 days. Kupffer cells were maintained in RPMI 1640 medium supplemented with 10% FBS and 1% antibiotic-antimycotic. LSECs were purified by MACS using anti-CD146 (cat. 130-092-007, Miltenyi Biotec, German) and anti-CD11b MACS beads. $CD146^+$ and $CD11b^-$ cells were used as previously described [3]. Primary hepatocytes were obtained by collagenase perfusion, followed by Percoll (cat. 14051ES60, Yeasen, Shanghai, China) density gradient centrifugation, as previously described [4]. Isolated hepatocytes were plated on rat collagen type I (cat. 354236, Coring, MA, USA)-coated dishes and maintained in Media 199 cell culture medium supplemented with 10% FBS and 1% antibiotic-antimycotic. A subset of cells was harvested after 24 hours and served as the quiescent control cells. All HSC cells were treated as indicated and harvested after 3-7 days, as indicated. Peripheral blood mononuclear cell (PBMCs) from human (cat. GS3701) and mice (GS3702, Genview, Shanghai, China) were assessed using respective commercial kit.

Measurement of serum GDNF concentration

A human GDNF ELISA kit (cat. DY212) from R&D (MN, USA) was used. A mouse GDNF ELISA kit was purchased from Boster Biological Technology Co. Ltd

(EK0935, Wuhan, China). 96-well microplates (R&D, cat. DY990) were coated with a capture antibody. After washing with wash buffer and blocking for 1 hour with reagent diluent, the samples were added and incubated for 2 hours at 37 °C. The detection antibody was added and incubated for 1 hour at 37 °C. Working streptavidin-HRP was then added for 20 minutes at 37°C. Substrate solution was added for 20 minutes at 37 °C, and stop solution (2N H_2SO4) was then added. The optical density was read at 450 nm using Varioscanlux (Thermo, MN, US).

Mice

Male C57/BL6 mice (18-20 g) were housed in an air-conditioned room at 25 ℃ with a 12 hour-dark/light cycle. Mice received humane care with unlimited access to a chow diet and water during the study. All of the study protocols complies with the current ethical considerations of Putuo Hospital, Shanghai University of Traditional Chinese Medicine's and HwaMei Hospital, University of Chinese Academy of Sciences Animal Ethic Committees. All animal procedures were conducted in accordance with Chinese laws and with the approval of the home office and local ethics committees.

For CCl_4-induced liver fibrosis, mice received three weekly intraperitoneal CCl_4 injections (0.25 ml/kg) for 6 weeks to induce chronic liver injury and were then sacrificed 2 days after the last injection. Olive oil was used as the vehicle control.

For the bile duct ligation (BDL) model, mice were anesthetized by the injection of ketamine and xylazine. After midline laparotomy, the common bile duct was ligated twice with 6-0 silk sutures, and the abdomen was closed. The sham operation was performed similarly, except that the bile duct was not ligated. After two weeks of sham and BDL operation, the mice were sacrificed and tissue and blood samples were harvested.

For the diet-induced NASH fibrosis model, mice were fed HFD (60% of calorie from fat, cat. D12492i, Research Diets, New Brunswick) for 14 weeks [5] or a methionine- and choline-deficient-diet (MCD) (cat. TP3006, Trophic, Nantong, China) for 8 weeks [6].

Ad-GDNF-virus and Ad-sgGDNF-virus injections.

Recombinant adenoviruses (10^6 pfu/ml each) comprising Gdnf sgRNA CRISPR adenovirus (cat. K4921721), scrambled sgRNA CRISPR adenovirus (cat. K020), Cas9 nuclease adenovirus (cat. K004), GDNF-His (cat. 093692A), and Adeno CMV Null (cat. 000047A) were purchased from Abm (Richmond, Canada). We amplified the adenoviruses in HEK293 cells, which were then centrifuged in a Sorvall LYNX 4,000 superspeed centrifuge (Thermo Scientific). Upon collection, the adenovirus preparations were desalted using PD-10 spin adapter columns (cat. 28-9262-94, GE Healthcare, UK) and stored at 10^{11} pfu/ml in HBSS.

Male C57BL/6 mice were i.p. injected with olive oil or CCl_4 three times a week for 6 weeks. Adenovirus injections (1×10^{11} pfu in 0.2 ml HBS per mouse) were performed via the tail vein at the end of the first, third, and fifth weekends [7]. In the BDL model, male C57BL/6 mice were injected as described above at 1 week after the sham- or BDL- operation, and the mice were sacrificed 1 week later.

CCl_4 mice (n=18) were randomly divided into the CCl_4-control Ab (IgG, Proteintech, cat. B900610), CCl_4-Ab1 (Abcam, cat. 18956), and CCl_4-Ab2 (Santa Cruz, cat. sc-13147) groups from the beginning of the second week of CCl_4 treatment. Three groups continued to receive weekly CCl_4 treatment in addition to the administration of either 50 μl of IgG, Ab1 or Ab2 (once a week, in total 3 times), which was administered i.p. at a dose of 400 ng/g BW dissolved in physiological saline [8]. At the end of the fourth week, all animals were sacrificed.

Measurement of serum ALT and AST concentrations. Mouse serum ALT and AST concentrations were determined by a Varioskan LUX (Thermo, CA) and using ALT and AST assay kit that were purchased from Jiangcheng (Nanjing, China).

Sirius red staining and quantification

Liver specimens were preserved in 4% paraformaldehyde and then dehydrated in a graded alcohol series. Then, the sections were embedded in paraffin blocks, cut into 5-μm-thick sections and placed on glass slides. The sections were stained with Sirius

red. To quantify Sirius red staining, images of five or six random fields of each section were taken. The collagen values are expressed as the percentage of the area of the section occupied by Sirius red staining using Image-Pro-plus (IPP) software (Media Cybernetics, MA, USA)

Immunohistochemical staining and quantification

After deparaffinization and dehydration, antigen retrieval was performed using microwave for 5 minutes before peroxidase quenching with 3% H_2O_2 in phosphate-buffered saline (PBS) for 15 minutes. Subsequently, the sections were blocked with 5% bovine serum albumin (BSA) for 30 minutes and then incubated with a primary antibody at a dilution ratio of 1:500 in PBS overnight at 4 ℃. The negative control was treated the same as the sample groups, except that primary antibodies were omitted in the incubation steps. The percentage of the area of the section occupied by positive staining using IPP software.

For double immunohistochemical staining, frozen sections were fixed in 1% paraformaldehyde (PFA) for 10 minutes and then washed 3 times with PBS. Sections were postfixed in precooled ethanol/acetone 2:1 for 5 minutes, washed 3 times with PBS washed and incubated in 5% BSA blocking solution for 30 minutes. Primary antibodies were added to the slides for 1 hour, and 1 drop of rabbit AP polymer and mouse HRP polymer was applied to the sections. Next, steps are DAB staining and 3 washes with PBST were performed, followed by incubation in permanent red working

solution for 20 minutes, mounting and analysis.

qPCR analysis

Total RNA was extracted using Trizol (Takara, Japan), followed by the reverse transcription of total RNA to cDNA with a PrimeScript RT reagents kit (perfect real time) from Takara (Shanghai, China). Subsequently, cDNA was subjected to quantitative real-time polymerase chain reaction (PCR) with the ABI ViiA™ 7Dx real-time PCR system (Life Technologies, NY, USA). The levels of the target mRNAs were normalized to that of 18S rRNA. The gene expression values are expressed as 2-ΔCt. PCR primer sequences were provided by Sangon (Shanghai, China) and are as presented in ***Supporting Table 1.***

Immunoblotting

Liver and cell lysates were prepared with ice-cold radioimmune precipitation assay buffer containing protease inhibitors. After protein quantification, the protein lysates were subjected to polyacrylamide gel electrophoresis and transferred onto Immobilon-P transfer membranes, which were then blocked and exposed to the corresponding antibodies. The blots were visualized by enhanced chemiluminescence (GE Healthcare Life Sciences) and digital images and densitometry were performed using a Bio-Rad system.

Cytoplasmic and nuclear protein extraction

The cells were washed twice followed by the addition of lysis buffer A (10 mM HEPES-KOH (pH 7.8), 10 mM KCl, 0.1 mM EDTA (pH 8.0)). Then, the cells were collected and centrifuged at 4 ℃ 5000 rpm for 5 minutes, and the supernatant was transferred as the cytoplasmic protein extract. To the remaining pellets was added lysis buffer C (50 mM HEPES-KOH (pH 7.8), 20% glycerol, 420 mM KCl, 0.1 mM EDTA (pH 8.0), 5 mM $MgCl_2$) followed by mixing, vortexing, and incubation on ice for 30 minutes and centrifugation at 4 ℃ and 14000 rpm for 10 minutes. Finally, the supernatants were transferred to a new tube as the nuclear protein extracts.

Molecular Docking

The crystal structure of the ALK5 extracellular region was obtained from the Protein Data Bank (PDB ID:2L5S), and GDNF structure was obtained from 3FUB. Prior to docking, the structures were both prepared with the built-in Molecular Operating Environment (MOE, Canada) method. The ALK5-GDNF complex model was constructed by the protein-protein docking method, as described previously[9]. Briefly, of ALK5 and GDNF complex was generated by rigid-body docking using PatchDock (http://bioinfo3d.cs.tau.ac.il/PatchDock/). Based on the shape complementarity of the soft molecular surface, PatchDock was used to determine the best starting candidate solutions. The PatchDock algorithm divided the Connolly dot surface representation of the proteins into convex, concave, and flat patches. Complementary patches were matched to generate candidate solutions. According to both geometric fit and atomic desolvation energy, the scoring function was utilized to

evaluate each candidate solution. The best docked candidate solutions were re-evaluated by FireDock (http://bioinfo3d.cs.tau.ac.il/FireDock/), on the basis of global energy, attraction van der Waals energy, repulsive van der Waals energy, atomic contact energy, insideness measurements, Coulomb electrostatics, and hydrogen and disulfide bonds. By restricting the side chains in interaction interface to small rigid-body movements, FireDock optimized and rescored candidate solutions and then produced the top solution of the complex structure. Molecular graphics for the best binding pose were generated using PyMOL (DeLano Scientific, http://www.pymol.org) and LigPlus.

Mutagenesis

The pcDNA3-ALK5 wild-type plasmid was purchased from Addgene (cat. 80876). The interaction of ALK5 and GDNF occurs mainly through His^{39} and Asp^{76}, so inactive ALK5 was generated by replacing His^{39} and Asp^{76} residues with Ala. Mutagenesis was performed using the KOD-Plus-Mutagenesis Kit (cat. SMK-101, Toyobo, Osaka, Japan) according to the manufacturer's instructions [10, 11] the following primers were also used: AKL5-His^{39}-F-GCGCCCTCTGTACAAAAGACAATTTTAC, AKL5-His^{39}-R-AGAAACACTGTAACGCCGTCG. AKL5-Asp^{76}-F-AATTTCAGCTATACACATGCTGtt, AKL5-Asp^{76}-R-GcCTTAATTCCACGAGATAGGccg.

Co-immunoprecipitation

For ALK5 and GDNF immunoprecipitation, we followed the Co-IP protocol as described previously [12, 13]. Cells were lysed with 1 ml lysis buffer containing protease inhibitors for 10 minutes at 4 ℃. After centrifugation at 12000 rpm for 15 minutes, the protein concentrations were measured, and equal amounts of lysate were used for immunoprecipitation. Immunoprecipitation was performed with different antibodies and protein A-Sepharose (GE Healthcare Bio-Sciences AB) for 1 hour at 4℃. Thereafter, the precipitants were washed three times, and the immune complexes were eluted with sample buffer for 5 minutes at 95 ℃. The immunoprecipitated proteins were then separated by SDS-PAGE.

Laser Confocal Microscopy

Tri-color immunofluorescence staining of human liver sections was performed with different antibody combinations as detailed in our previous report[2]. For instance, for GDNF, ALK5, and α-SMA tri-color staining, liver sections were first incubated with rabbit anti-GDNF for 1 hour at 37 ℃, then with Cy2-conjugated goat anti rabbit secondary antibody (cat. 111-225-144, Jackson ImmunoResearch, PA, USA); after three PBS washes, the liver sections were incubated with monoclonal anti-α-SMA antibody for 1 hour at 37 ℃. DyLight 405-conjugated donkey anti-mouse secondary antibody (cat.715-475-150, Jackson ImmunoResearch, PA, USA) was added and incubated for 30 minutes at room temperature. After washing, the sections were incubated with goat-anti ALK5 antibody for 1 hour at 37 ℃, followed by rhodamine

(TRITC)-conjugated donkey anti-goat secondary antibody (cat.705-025-003, Jackson ImmunoResearch, PA, USA) at room temperature for 30 minutes; then the sections were then covered with mounting medium. The slides were visualized using a Zeiss confocal LSM 5880 microscope (Zeiss) and processed using Zeiss LSM Image Examiner software (Zeiss).

ChIP analysis

Chromatin immunoprecipitation (Ch-IP) assays were performed with a Magna Ch-IP HiSens Kit (Cat. 17-10460, Merk, Darmstadt, Germany) according to the manufacturer's instructions. Chromatin was immunoprecipitated with IgG or anti-Smad2/3 antibodies. DNA was extracted and PCR was performed to assess the bound sequences. Forward 5'-GAGAAGCGAACTGGGGACTT-3', Reverse, 5'-ATCTTAAAGTCCCGTCCGGC-3'.

Statistics. The values are expressed as the mean ± SD. The experiments were performed using 3 biological replicates for each treatment. One-way analysis of variance (ANOVA) with the nonparametric Kruskal-Wallis test was used for comparison of multiple groups, and the Student's t-test Mann-Whiney test was used to examine differences between two groups. The nonparametric correlation (Spearman) was analyzed between GDNF and other variables. GraphPad Prism software version 6.0 (GraphPad Software, San Diego, CA, USA) was used. Statistical significance was defined as $P<0.05$.

Supporting Discussion

GDNF – a trophic factor in neural cells

GDNF was originally identified based on its ability to maintain embryonic ventral midbrain dopaminergic neuron survival *in vitro* [14]. Mice with a disrupted GDNF gene display defects in primary sensory, sympathetic and motor neurons and die shortly after birth due to the absence of renal function [15]. Other studies have described protective effects of GDNF in animal models of Parkinson's disease [16], and GDNF-transduced MSCs are protective against inflammation-induced Parkinsonism [17]. Subsequently, gene therapy or cell therapy with GDNF gene-transduced BMSCs has improved the recovery process in a rat model of spinal cord injury [18]. These data indicate a protective role for GDNF in neural physiology. Furthermore, GDNF injection into the ventral tegmental area, a dopaminergic brain region important for addiction, inhibits certain biochemical adaptations to cocaine or morphine [19], and clinical studies show that GDNF levels are increased in the parietal cortex and plasma of patients with depressive disorder [20]. In addition to its neuronal functions, increased GDNF levels have been reported following exposure to cytotoxic agents, including radiation [21], and in cancer cells as a pro-angiogenic factor [22].

Supporting Tables

S-Table 1 human and mouse primers used for PCR

Gene	***Primer sequences (5'-3')***
Human primers	
hGDNF-F	GCAGTTAAGACACAACCCCG
hGDNF-R	AGTTATGGGATGTCGTGGCT
hα-SMA-F	CAAAGCCGGCCTTACAGAG
hα-SMA-R	AGCCCAGCCAAGCACTG
18S rRNA-F	GTAACCCGTTGAACCCCATT
18S rRNA-R	CCATCCAATCGGTAGTAGCG
hCol1A1-F	TAGGCCATTGTGTATGCAGC
hCol1A1-R	ACATGTTCAGCTTTGTGGACC
hRet-F	AAGCATCCCTCGAGAAGTAGA
hRet-R	CTAGCCGCAGTCCCTCC
hALK5-F	GAGCCCATCTGTCACACAAGT
hALK5-R	GCTGCTCCTCCTCGTGCT
hGRFα1-F	TTGTTCCCTTTGGGAATGTG
hGFRα1-R	TGGAGGATTCCCCATATGAA
Mice primers	***Primer sequences (5'-3')***
m*Alk5*-F	GCAAAGACCATCTGTCTCACA
m*Alk5*-R	CTCCTCATCGTGTTGGTGG
m*Gdnf*-F	CGTCATCAAACTGGTCAGGA
m*Gdnf*-R	CCGGTAAGAGGCTTCTCG
m*Ret*-F	CCAGCTGGCTGGTCTACATA
m*Ret*-R	GAAGCTGATTTTGCTCCTGC
m*Tnfα*-F	ATGAGAGGGAGGCCATTTG
m*Tnfα*-R	CAGCCTCTTCTCATTCCTGC
m*Timp1*-F	TGGGGAACCCATGAATTTAG
m *Timp1*-R	ATCTGGCATCCTCTTGTTGC
m*Cd68*-F	ACATTGTATTCCACCGCCAT
m *Cd68*-R	CATCCCCACCTGTCTCTCTC
m*Ccl2*-F	ATTGGGATCATCTTGCTGGT
m*Ccl2*-R	CCTGCTGTTCACAGTTGCC
m*Col1α1*-F	TAGGCCATTGTGTATGCAGC
m*Col1α1*-R	ACATGTTCAGCTTTGTGGACC
m*Mmp9*-F	GTGGTTCAGTTGTGGTGGTG
m *Mmp9*-R	CCCGCTGTATAGCTACCTCG
mα- *Sma* -F	GTTCAGTGGTGCCTCTGTCA
mα-*Sma*-R	ACTGGGACGACATGGAAAAG
m*Mmp2*-F	GACGGCATCCAGGTTATCAG
m*Mmp2*-R	TGCAGGAGACAAGTTCTGGA

Abbreviations: h, human; m, mouse; α-SMA, smooth muscle actin; CCL, C-C motif chemokine ligand; Col1A1, collagen type 1 alpha 1 chain; GDNF, glial cell line-derived neurotrophic factor, GFRα1, GDNF family receptor alpha 1; MMP, matrix metalloprotein; Ret, Ret proto-oncogene; TIMP1, tissue inhibitor of metalloproteinases 1; TNF, tumor necrosis factor.

S-Table 2. NAFLD patient characteristics

Variable	F0/1(n=11)	F2/3 (n=7)	*P*- value
Age (years)	40.50 ±16.06	40.85±12.45	0.260
Gender (F/M)	8/3	4/3	0.494
BMI(kg/m^2)	24.44±2.74	25.18±2.03	0.128
ALT (U/L)	90.82±78.47	116.70±105.23	0.539
AST (U/L)	50.34±31.42	74.72±36.99	0.308
Glucose (mmol/L)	4.61±0.70	4.70±0.37	0.135
Cr (μmol/L)	68.59±10.90	65.13±12.69	0.168
BUN (mmol/L)	4.64±0.57	5.32±1.21*	0.043
TG (mmol/L)	1.50±0.41	1.37±0.52	0.105
TC (mmol/L)	4.74±1.00	5.71±0.97	0.940
WBC (10^9/L)	7.08±1.52	6.29±2.47	0.130
Neutrophils (%)	55.07±5.69	52.83±10.83*	0.021
RBC (10^{12}/L)	5.01±0.37	4.55±0.41	0.540

The data are expressed as the mean ± standard deviation.

ALT, alanine aminotransferase; AST, aspartate aminotransferase; BUN, blood urea nitrogen; Cr creatinine; RBC, red blood cell; TC, total cholesterol; TG, triglyceride; WBC, white blood cell count. *p<0.05, compared to F0/1 stage patient.

S-Table 3. Alcoholic liver disease patient characteristics

Variable	Health control (HC, n=30)	Alcohol hepatitis (AH, n=26)	Alcohol cirrhosis (AC, n =11)	*P*- value
Age (years)	42.8±6.2	58.9±8.7	58.4±7.5	0.478
Gender (F/M)	20/10	25/1	11/0	0.003
ALT (U/L)	8.67±3.40***	123.00±144.21$^{\#\#\#}$	78.09±93.81	0.000
AST (U/L)	17.17±2.94*	86.50±94.62$^{\#}$	129.63±173.13$^{\#\#\#}$	0.001
TBiL (μmol/L)	N.D	39.11±46.94	179.18±234.48***	<0.001
Alb (g/L)	N.D	38.08±5.21	29.81±7.7*	0.012
Cr (μmol/L)	54.61±8.57***	88.80±48.91$^{\#\#\#}$	98.45±49.56$^{\#\#\#}$	0.000
BUN (mmol/L)	3.68±1.24	5.10±3.42	8.18±5.49$^{*\#\#\#}$	0.001
TG (mmol/L)	N.D	4.53±1.43	3.40±3.27	0.270
TC (mmol/L)	N.D	1.71±0.77	1.04±0.52	0.327
HDL (mmol/L)	N.D	1.02±0.38	0.92±0.55	0.091
LDL (mmol/L)	N.D	2.89±1.00	2.23±2.51	0.269
HA （ng/mL）	N.D	191.94±208.91	673.57±455.55***	<0.001
PCIII (ng/mL)	N.D	10.62±5.30	18.36±11.76***	<0.001
LN （ng/mL）	N.D	65.13±50.62	248.95±233.54**	0.001
CIV （ng/mL）	N.D	79.95±70.24	118.20±63.11	0.791
WBC (10^9/L)	8.04±10.04	6.24±1.81	6.89±2.18	0.617
Neutrophils (%)	61.79±10.48	55.27±12.31	66.51±16.76*	0.021
RBC (10^{12}/L)	4.43±0.47***	4.39±0.76$^{\#\#\#}$	3.20±0.87$^{\#\#\#}$	0.000
PT (Sec)	N.D	13.05±0.88	18.53±6.11***	<0.001
INR	N.D	1.01±0.09	1.58±0.66***	<0.001
AFP (μg/L)	N.D	4.74±3.27	7.02±7.30**	0.005

The data are expressed as the mean ± standard deviation. AFP, alpha fetoprotein; Alb, albumin; ALT, alanine aminotransferase; AST, aspartate aminotransferase; BUN, blood urea nitrogen; Cr creatinine; HA, hyaluronic acid; HDL, high-density lipoprotein cholesterol; INR, international normalized ratio; CIV, type IV collagen; LN, Laminin; PCIII, type III procollagen; RBC, red blood cell; TBil, total bilirubin; TC, total cholesterol; TG, triglyceride; TP, total protein; PT, prothrombin time; WBC, white blood cell count. $^{\#}$p<0.05, $^{\#\#}$p <0.01, $^{\#\#\#}$p<0.001 compared to healthy controls. *p <0.05, **p<0.01, ***p<0.001 compared to alcohol hepatitis patients.

Supporting Figures and Legends

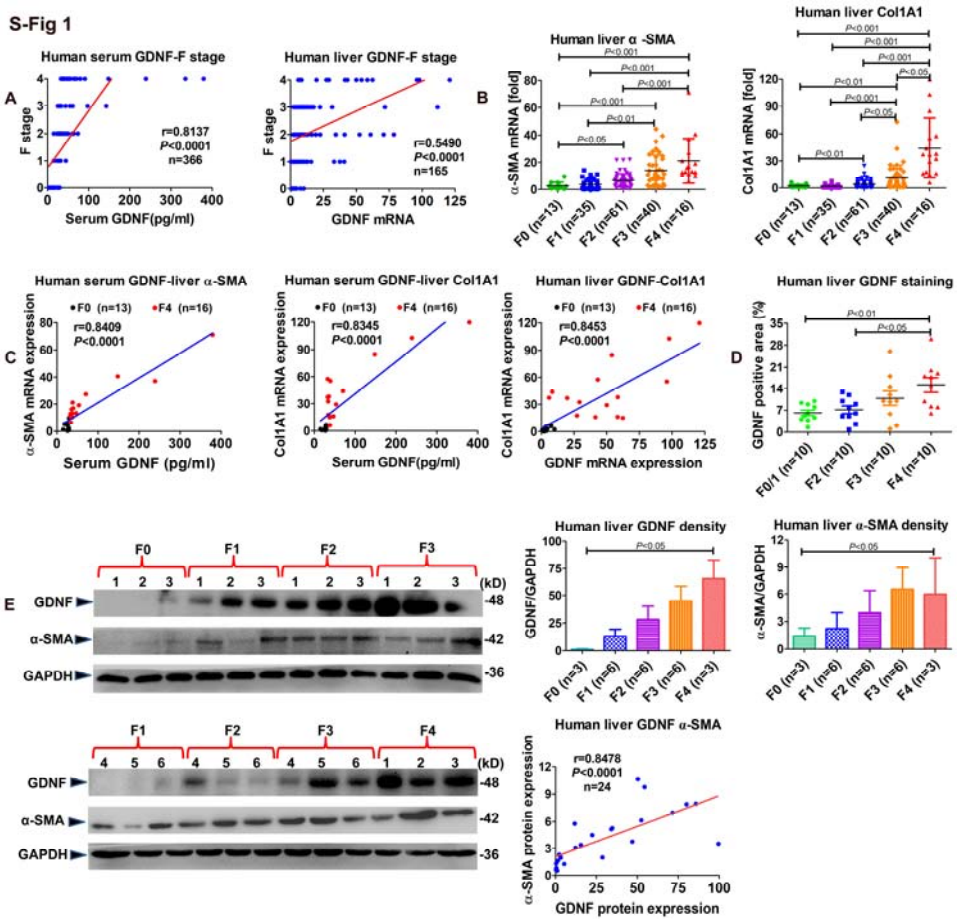

S-figure 1. GDNF levels correlate significantly with liver fibrosis in human patients.

A, Correlation analysis between GDNF levels in serum, mRNA in the liver and F stage fibrosis in the examined patients.

B, α-SMA and Col1A1 mRNA expression in 165 human liver specimens was examined by real-time PCR. The levels of target mRNAs were normalized to 18S rRNA (F0=13; F1=35; F2=61; F3=40; F4=16).

C, Correlation analysis between GDNF concentrations in serum and α-SMA/Col1A1 mRNA expression.

D, Semiquantitative analysis of GDNF immunohistochemistry.

E, GDNF and α-SMA expression in 24 human liver specimens was examined by immunoblot analysis (F0=3 F1=6; F2=6; F3=6; F4=3). Correlation analysis between GDNF and α-SMA protein expression in the examined patients collective is presented.

Bars indicate the mean ± SD of three independent experiments. One-way ANOVA with the nonparametric Kruskal-Wallis test analysis was used in B, D, and E, and nonparametric correlation (Spearman) two-tailed test was used in A, C and E.

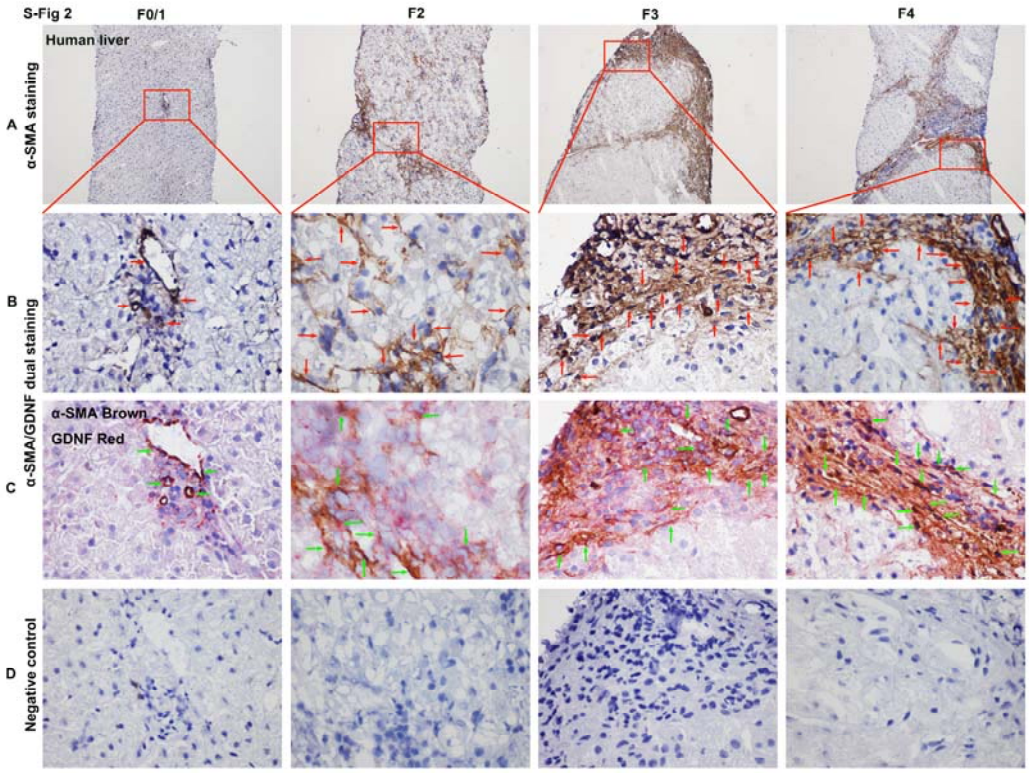

S-figure 2. GDNF is mainly expressed in α-SMA-positive cells in progressed stages of human liver fibrosis.

A, Frozen human liver biopsy sections with α-SMA immunohistochemical staining (original magnifications, x 100), (n=10 per group).

B, The boxed area in A shows a magnification of x 600; red arrows indicate α-SMA positive staining.

C, The same location as in B with α-SMA and GDNF double immunohistochemical staining using serial sections (original magnifications, x 600); green arrows indicate α-SMA and GDNF double positive staining.

D, Negative control showing the same location as the upper row (original magnifications, x 600).

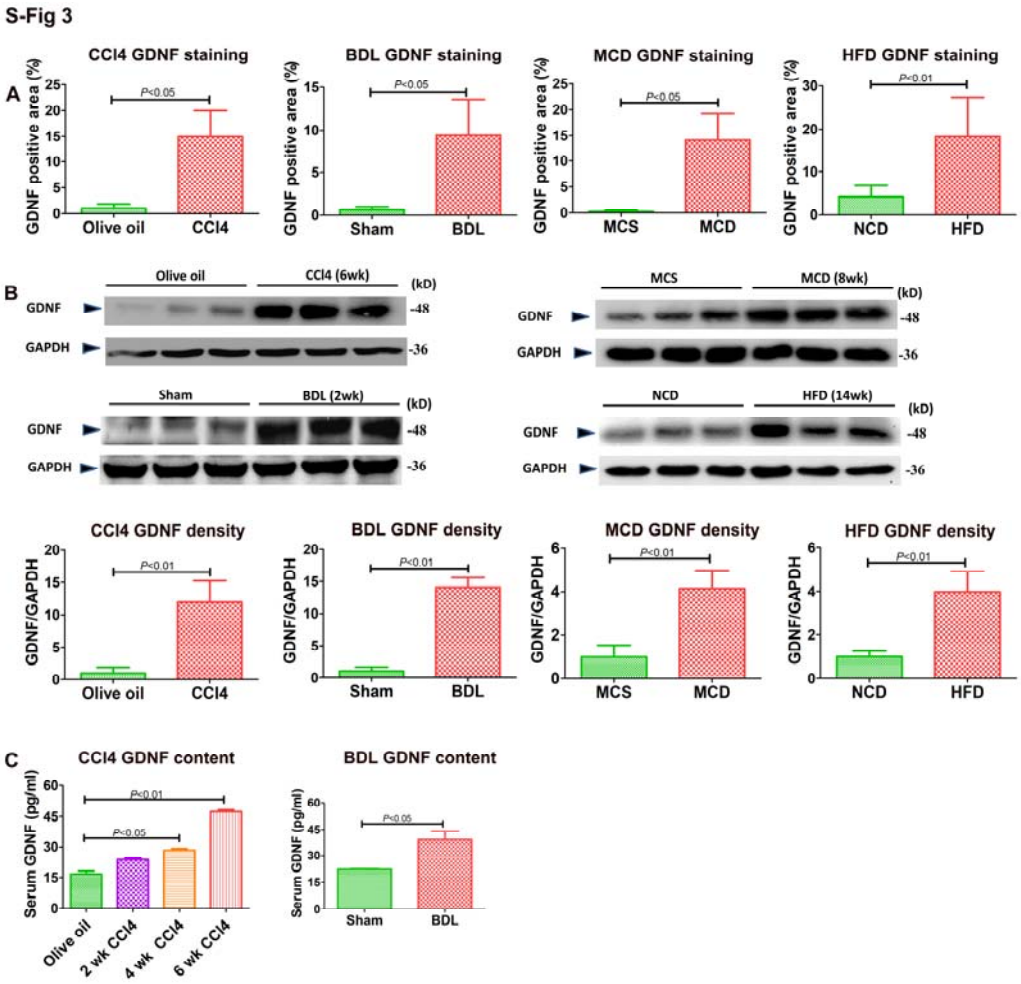

S-figure 3. GDNF is up-regulated in different fibrosis mouse models

A, Quantification of GDNF positive area from figure 2.

B, Hepatic GDNF protein expression in mice with fibrosis from CCl_4, BDL, MCD and HFD.

C, Serum GDNF concentrations in CCl_4 and BDL-induced liver fibrosis examined using ELISA analysis.

Bars indicate the mean ± SD of three independent experiments; n=5 per group. One-way ANOVA with the nonparametric Kruskal-Wallis test was used in C. t-test with the nonparametric Mann-Whiney test was used in A-C.

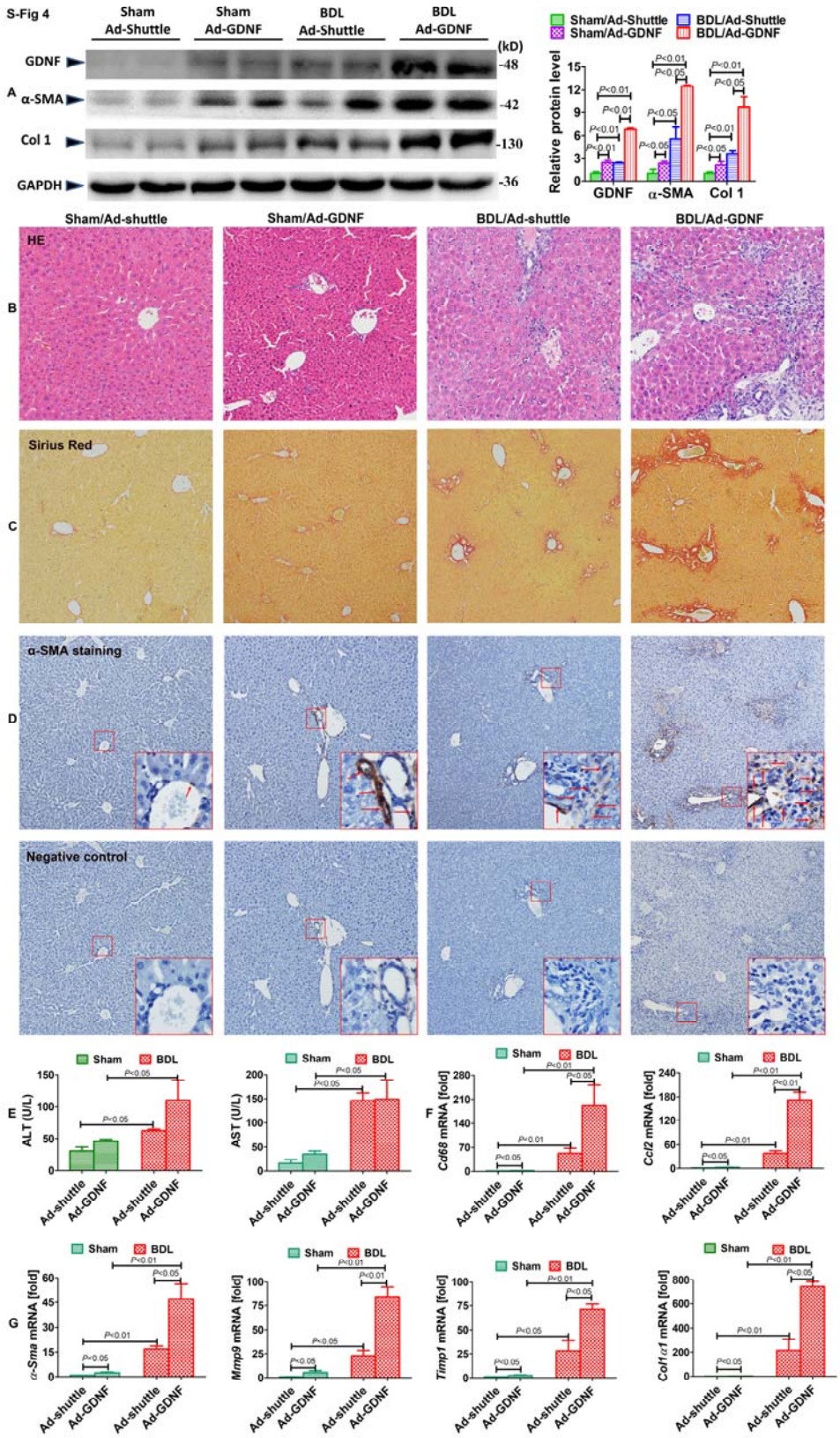

S-figure 4. GDNF overexpression exacerbates experimental liver fibrosis in BDL mice.

Comparative analysis of sham and BDL mice treated with Ad-GDNF *vs* Ad-shuttle treatment (n=5 for each group).

A, GDNF, α-SMA and Col 1 were examined by immunoblotting in CCl_4-induced liver fibrosis.

B-D, Representative images of HE (B), Sirius red (C), and α-SMA immunohistochemistry, and the negative control showing all the same location (D) (original magnification, x 100); red arrows indicate α-SMA-positive staining.

E, ALT and AST levels in serum samples from mice.

F, mRNA expression levels of pro-inflammatory cytokines *Cd68* and *Ccl2*, as well as G, mRNA expression levels of fibrogenic markers, all examined by real-time PCR.

Bars indicate the mean ± SD of three independent experiments; n=5 per group. One-way ANOVA with the nonparametric Kruskal-Wallis test was used in A, E-G.

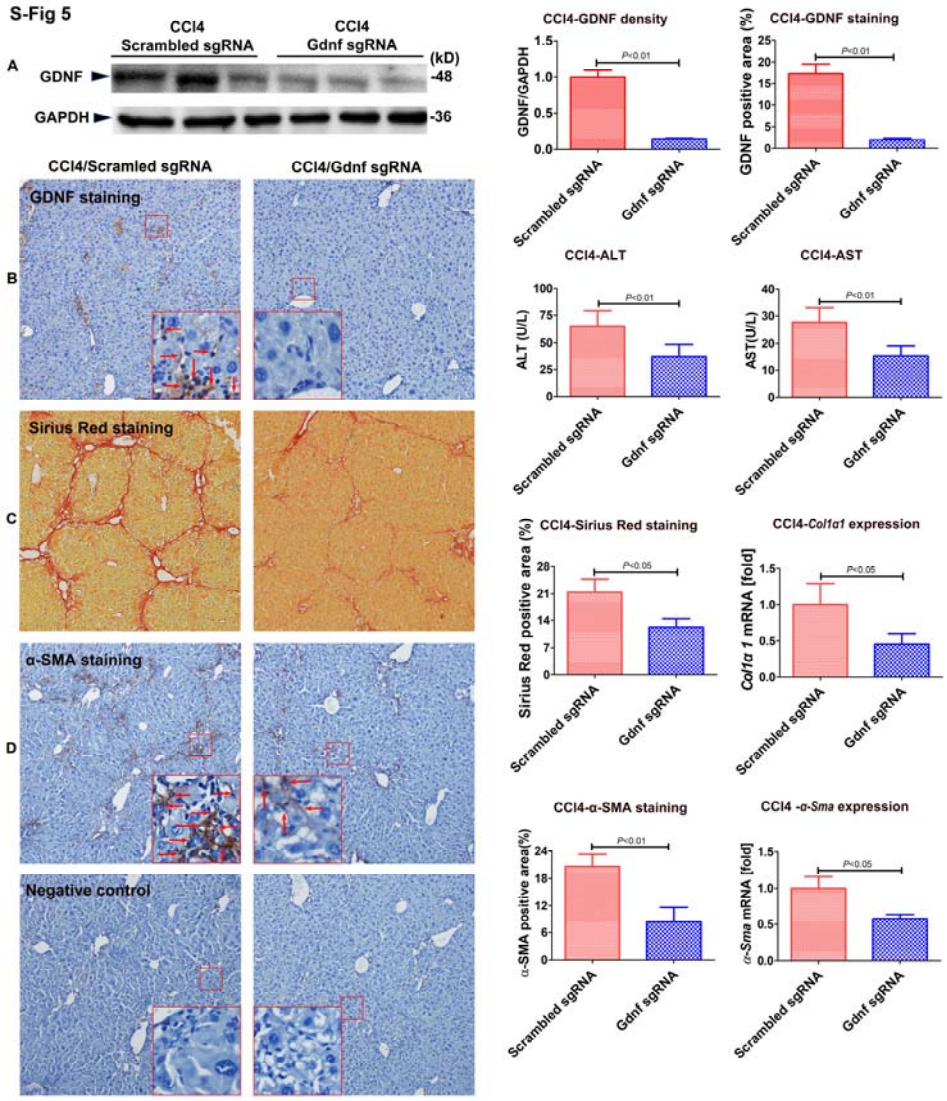

S-figure 5. GDNF depletion alleviates HSC activation and CCl_4-induced liver fibrosis in mice.

A, Western blots used for GDNF knockdown detection.

B, GDNF staining, ALT, and AST levels were examined in CCl_4-induced liver fibrosis in mice treated with scrambled or *Gdnf* sgRNA/Cas9 (original magnification, x 100), the larger boxes show magnification of x 600.

C, Sirius red staining, semi-quantification of positive areas, and *Col1α1* mRNA expression analysis were performed (original magnification, x 100).

D, α-SMA immunohistochemical staining and negative control showing the same area, semi-quantification and *α-Sma* mRNA expression as determined by real-time PCR analysis in CCl_4-induced liver fibrosis in mice treated with *Gdnf* or scrambled sgRNA/Cas9 (original magnification, x 100). The enlarged boxes show magnifications of x 600 of the small boxes.

Bars indicate the mean ± SD of three independent experiments; n=5 per group. The t-test with the nonparametric Mann-Whitney test was used. The red arrow indicates positive staining.

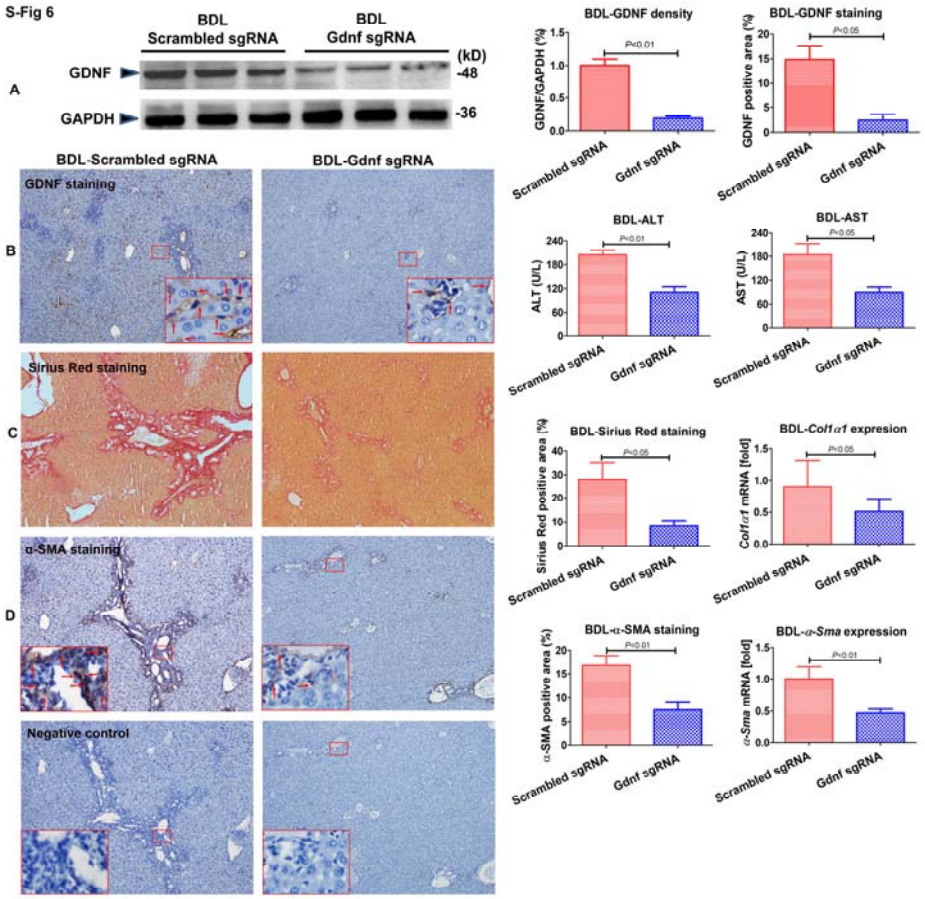

S-figure 6. GDNF depletion alleviates BDL-induced liver fibrosis in mice

Comparative analysis of BDL mice treated with Gdnf directed or scrambled sgRNA/Cas9.

A, Hepatic GDNF expression in BDL-induced liver fibrosis was examined by immunoblotting.

B, Hepatic GDNF staining, ALT, and AST levels in BDL-induced liver fibrosis upon treatment with scrambled or *Gdnf* directed sgRNA/Cas9 (original magnification, x 100); the larger boxes show magnifications of x 600 from the small boxes.

C, Sirius red staining semi-quantification and *Col1α1* mRNA, examined by real-time PCR analysis in BDL-induced liver fibrosis in mice upon treatment with *Gdnf*

targeting or scrambled sgRNA/Cas9 (n=5 for each group) (original magnification, x 100), the larger boxes show magnifications of x 600 from the small boxes.

D, α-SMA immunohistochemical staining and semi-quantification, as well as *α-Sma* mRNA levels, determined by real-time PCR analysis in BDL-induced liver fibrosis in mice treated with Gdnf directed or scrambled sgRNA/Cas9 (n=5 for each group) (original magnification, x 100), the larger boxes show magnifications of x 600 from the small boxes.

Bars indicate the mean ± SD of three independent experiments; n=5 per group. The t-test with the nonparametric Mann-Whitney test was used. The red arrow indicates positive staining.

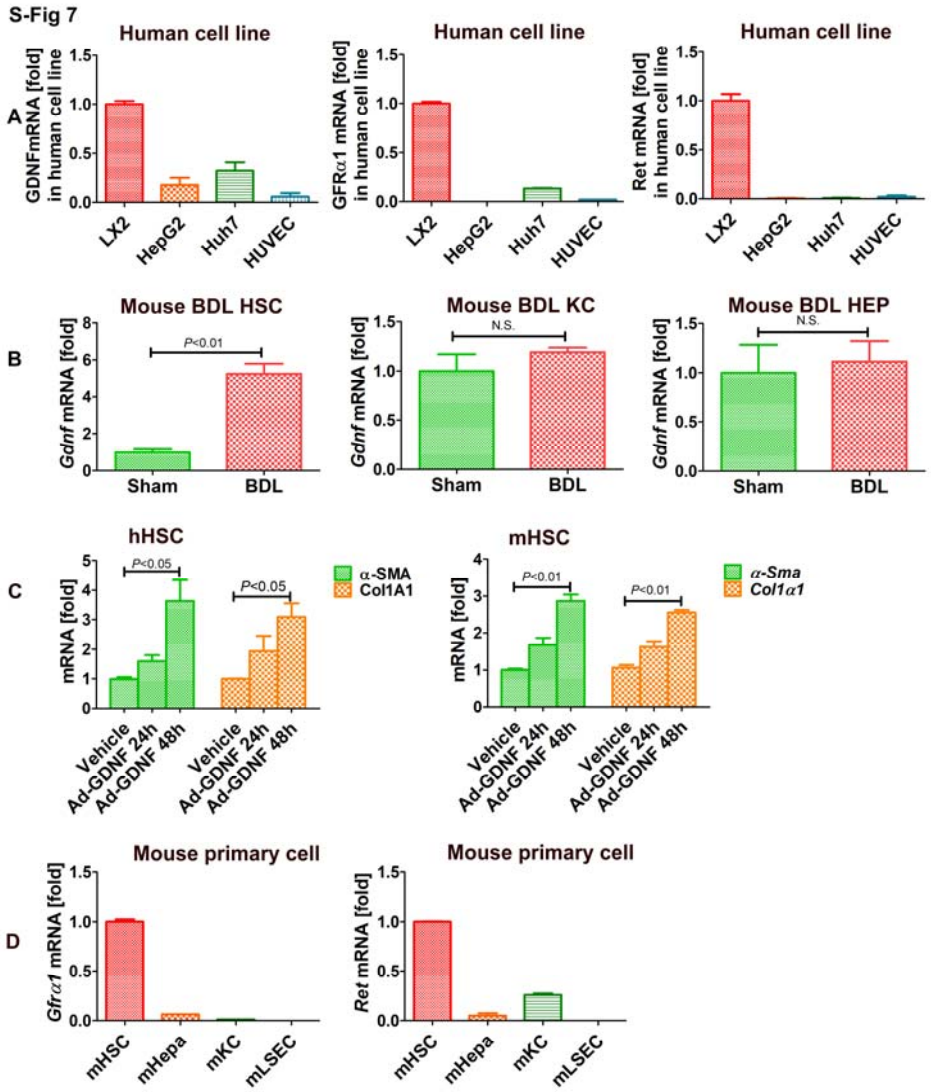

S-figure 7. GDNF and its receptor expression in human cell lines and mouse primary liver cells

A, Real-time PCR for GDNF, GFRα1 and Ret mRNA in human cell lines.

B, *Gdnf* mRNA in cells from mice with BDL. Bars indicate the mean ± SD of three independent experiments, n=3 per group. The t-test with the nonparametric Mann-Whitney test was used.

C, Expression of α-SMA and Col 1A1 was increased significantly after Ad-GDNF treatment for 48 hours, as determined by real-time PCR analysis. Bars indicate the

mean ± SD of three independent experiments, n=3 per group. The t-test with the nonparametric Mann-Whitney test was used.

D, Real-time PCR for *Gfrα1* and *Ret* mRNA in primary liver cells from normal mice.

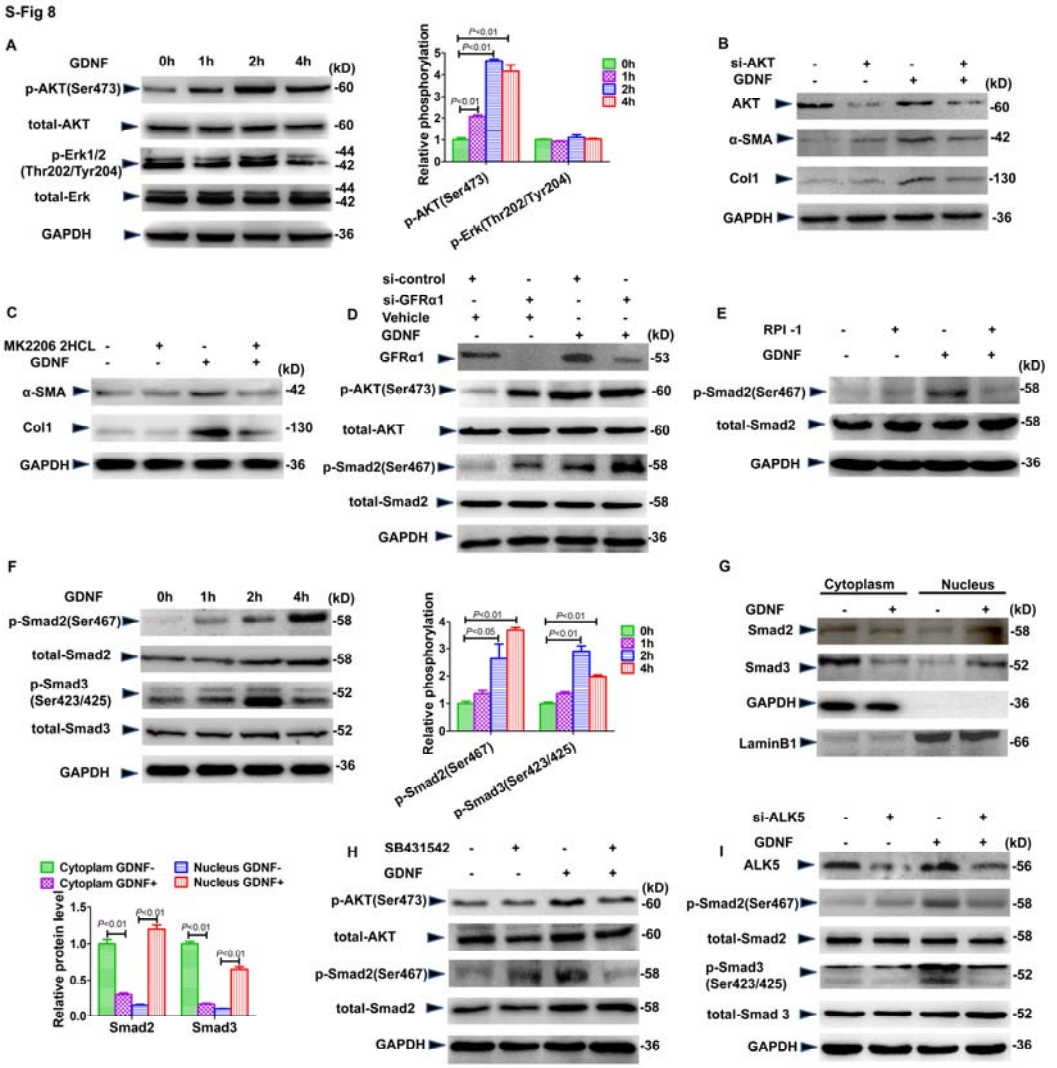

S-figure 8. GDNF induces HSC activation via the ALK5/Smad pathway.

A, Western blots for (p-)AKT and (p-)Erk and semiquantifications of bands. LX2 cells were treated with GDNF (10 ng/ml) for the indicated times.

B, Western blots for α-SMA and Col 1. LX2 cells were transfected with AKT siRNA for 12 hours and then treated with 10 ng/ml GDNF for an additional 48 hours.

C, Western blots for α-SMA and Col 1. LX2 cells were treated with MK2206 2HCL (0.5 μM) for 1 hour, then treated with GDNF for an additional 48 hours.

D, Western blots for (p-)AKT and (p-)Smad2. LX2 cells were transfected with GFRα1

siRNA for 48 hours and then treated with GDNF (10 ng/ml) for an additional 2 hours.

E, Western blots for (p-)AKT and (p-)Smad2. LX2 cells were treated with RPI-1 (60 μM) for 1 hour and then treated with GDNF (10 ng/ml) for additional 2 hours.

F, Western blots for (p-)Smad2, pSmad3, and semiquantification of bands. LX2 cells were treated with GDNF (10 ng/ml) as indicated.

G, Western blots for cytoplasmic and nuclear Smad2 and Smad3. LX2 cells were treated with GDNF (10 ng/ml) for 2 hours, and the nuclear and cytoplasmic proteins were then extracted as described in supporting material and methods.

H, Western blots for (p-)AKT and (p-)Smad2. LX2 cells were treated with SB431542 (10 μM) for 1 hour, then treated with GDNF (10 ng/ml) for an additional 2 hours.

I, Western blots for (p)-Smad2 and (p)-Smad3. LX2 cells were transfected with ALK5 siRNA for 12 hours, and then treated with GDNF (10 ng/ml) for an additional 48 hours.

Bars indicate the mean ± SD of three independent experiments, n=3 per group. One-way ANOVA with the nonparametric Kruskal-Wallis test was used in A, F, and G.

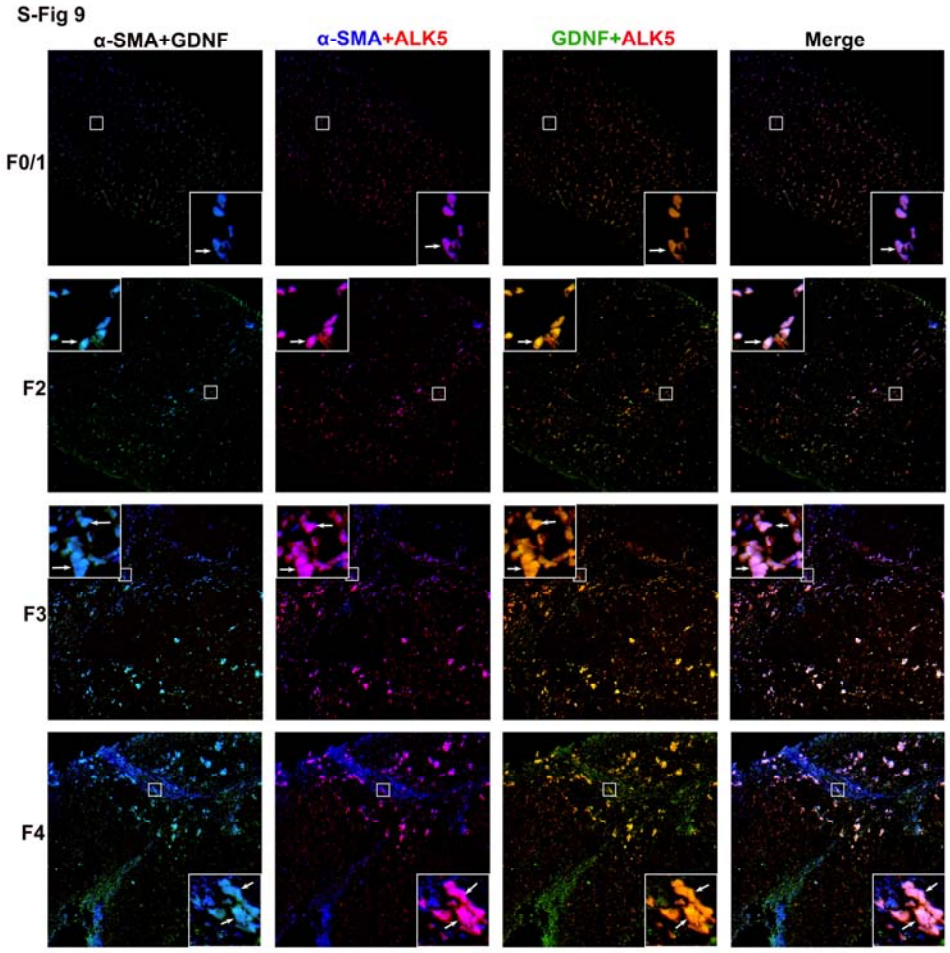

S-figure 9. GDNF, ALK5, and α-SMA colocalize in human liver fibrosis. Representative images of paraffin sections from patients with various stages of liver fibrosis are presented. GDNF (green), ALK5 (red) and α-SMA (blue) (original magnification, x 100); the arrows denote colocalization. The boxed area was enlarged and is presented as an inset (magnification, x 800), (n=5 per group).

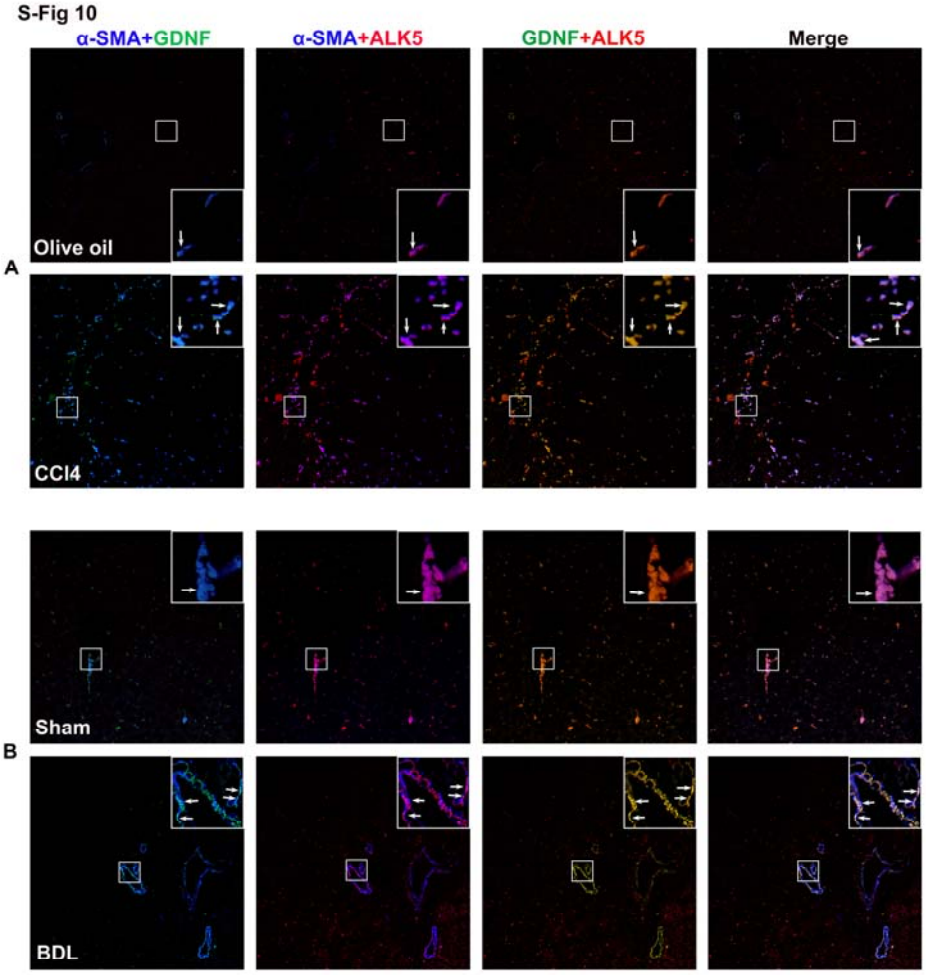

S-figure 10. GDNF, ALK5, and α-SMA colocalize in mouse liver fibrosis

Representative images of paraffin sections from CCl_4-(A) and BDL- (B) induced liver fibrosis as indicated by immunostaining for GDNF (green), ALK5 (red) and α-SMA (blue) (original magnification, x100); arrows denote colocalization. The boxed area was enlarged and is presented as inset (magnification, x 800), (n=5 per group).

References:

1 Seki E, De Minicis S, Osterreicher CH, Kluwe J, Osawa Y, Brenner DA*, et al.* TLR4 enhances TGF-beta signaling and hepatic fibrosis. Nat Med 2007;**13**:1324-32.

2 Liu C, Tao Q, Sun M, Wu JZ, Yang W, Jian P*, et al.* Kupffer cells are associated with apoptosis, inflammation and fibrotic effects in hepatic fibrosis in rats. Lab Invest 2010;**90**:1805-16.

3 Meyer J, Lacotte S, Morel P, Gonelle-Gispert C, Buhler L. An optimized method for mouse liver sinusoidal endothelial cell isolation. Exp Cell Res 2016;**349**:291-301.

4 Kodama Y, Taura K, Miura K, Schnabl B, Osawa Y, Brenner DA. Antiapoptotic effect of c-Jun N-terminal Kinase-1 through Mcl-1 stabilization in TNF-induced hepatocyte apoptosis. Gastroenterology 2009;**136**:1423-34.

5 Luo X, Li H, Ma L, Zhou J, Guo X, Woo SL*, et al.* Expression of STING Is Increased in Liver Tissues From Patients With NAFLD and Promotes Macrophage-Mediated Hepatic Inflammation and Fibrosis in Mice. Gastroenterology 2018;**155**:1971-84 e4.

6 Loyer X, Paradis V, Henique C, Vion AC, Colnot N, Guerin CL*, et al.* Liver microRNA-21 is overexpressed in non-alcoholic steatohepatitis and contributes to the disease in experimental models by inhibiting PPARalpha expression. Gut 2016;**65**:1882-94.

7 Han CY, Koo JH, Kim SH, Gardenghi S, Rivella S, Strnad P*, et al.* Hepcidin inhibits Smad3 phosphorylation in hepatic stellate cells by impeding ferroportin-mediated regulation of Akt. Nat Commun 2016;**7**:13817.

8 Koyama Y, Wang P, Liang S, Iwaisako K, Liu X, Xu J*, et al.* Mesothelin/mucin 16 signaling in activated portal fibroblasts regulates cholestatic liver fibrosis. J Clin Invest 2017;**127**:1254-70.

9 Schneidman-Duhovny D, Inbar Y, Nussinov R, Wolfson HJ. PatchDock and SymmDock: servers for rigid and symmetric docking. Nucleic Acids Res 2005;**33**:W363-7.

10 Hashimoto H, Nishioka M, Fujiwara S, Takagi M, Imanaka T, Inoue T*, et al.* Crystal structure of DNA polymerase from hyperthermophilic archaeon Pyrococcus kodakaraensis KOD1. J Mol Biol 2001;**306**:469-77.

11 Mizuguchi H, Nakatsuji M, Fujiwara S, Takagi M, Imanaka T. Characterization and application to hot start PCR of neutralizing monoclonal antibodies against KOD DNA polymerase. J Biochem 1999;**126**:762-8.

12 Xie F, Jin K, Shao L, Fan Y, Tu Y, Li Y*, et al.* FAF1 phosphorylation by AKT accumulates TGF-beta type II receptor and drives breast cancer metastasis. Nat Commun 2017;**8**:15021.

13 Liu C, Chen X, Yang L, Kisseleva T, Brenner DA, Seki E. Transcriptional repression of the transforming growth factor beta (TGF-beta) Pseudoreceptor BMP and activin membrane-bound inhibitor (BAMBI) by Nuclear Factor kappaB (NF-kappaB) p50 enhances TGF-beta signaling in hepatic stellate cells. J Biol Chem 2014;**289**:7082-91.

14 Lin LF, Doherty DH, Lile JD, Bektesh S, Collins F. GDNF: a glial cell line-derived neurotrophic factor for midbrain dopaminergic neurons. Science 1993;**260**:1130-2.

15 Cacalano G, Fariñas I, Wang LC, Hagler K, Forgie A, Moore M*, et al.* GFRα1 Is an Essential Receptor Component for GDNF in the Developing Nervous System and Kidney. Neuron 1998;**21**:53-62.

16 Yue P, Miao W, Gao L, Zhao X, Teng J. Ultrasound-Triggered Effects of the Microbubbles Coupled to GDNF Plasmid-Loaded PEGylated Liposomes in a Rat Model of Parkinson's Disease. Front Neurosci 2018;**12**:222.

17 Hoban DB, Howard L, Dowd E. GDNF-secreting mesenchymal stem cells provide localized neuroprotection in an inflammation-driven rat model of Parkinson's disease. Neuroscience 2015;**303**:402-11.
18 Shahrezaie M, Mansour RN, Nazari B, Hassannia H, Hosseini F, Mahboudi H*, et al.* Improved stem cell therapy of spinal cord injury using GDNF-overexpressed bone marrow stem cells in a rat model. Biologicals 2017;**50**:73-80.
19 Messer CJ, Eisch AJ, Carlezon WA, Jr., Whisler K, Shen L, Wolf DH*, et al.* Role for GDNF in biochemical and behavioral adaptations to drugs of abuse. Neuron 2000;**26**:247-57.
20 Park YM, Lee BH. Alterations in Serum BDNF and GDNF Levels after 12 Weeks of Antidepressant Treatment in Female Outpatients with Major Depressive Disorder. Psychiatry Investig 2018;**15**:818-23.
21 Huber RM, Lucas JM, Gomez-Sarosi LA, Coleman I, Zhao S, Coleman R*, et al.* DNA damage induces GDNF secretion in the tumor microenvironment with paracrine effects promoting prostate cancer treatment resistance. Oncotarget 2015;**6**:2134-47.
22 Zhong Z, Gu H, Peng J, Wang W, Johnstone BH, March KL*, et al.* GDNF secreted from adipose-derived stem cells stimulates VEGF-independent angiogenesis. Oncotarget 2016;**7**:36829-41.